Journal of Hazardous Materials 276 (2014) 112–119

Contents lists available at ScienceDirect

Journal of Hazardous Materials

journal homepage: www.elsevier.com/locate/jhazmat

Biosorption and biodegradation of triphenyltin by *Stenotrophomonas maltophilia* and their influence on cellular metabolism

Jiong Gao, Jinshao Ye*, Jiawen Ma, Litao Tang, Jie Huang

Key Laboratory of Water/Soil Toxic Pollutants Control and Bioremediation of Guangdong Higher Education Institutes, School of Environment, Jinan University, Guangzhou 510632, Guangdong, China

HIGHLIGHTS

- TPT was removed by the joint effect of biosorption, degradation and accumulation.
- TPT intracellularly degraded to produce diphenyltin and monophenyltin successively.
- TPT increased Cl^-, Na^+, arabinose, glucose and protein release.
- TPT increased the cellular membrane permeability.
- K^+ and PO_4^{3-} use, and intracellular protein level declined during TPT degradation.

ARTICLE INFO

Article history:
Received 5 January 2014
Received in revised form 27 April 2014
Accepted 11 May 2014
Available online 16 May 2014

Keywords:
Biosorption
Biodegradation
Triphenyltin
Stenotrophomonas maltophilia

ABSTRACT

Triphenyltin (TPT), an endocrine disruptor, is polluting the global environment through its worldwide use. However, information concerning the mechanisms of TPT biodegradation and cellular metabolism is severely limited. Therefore, these processes were elucidated through experiments involving TPT biosorption and degradation, intracellular metabolite analysis, nutrient use, ion and monosaccharide release, cellular membrane permeability and protein concentration quantification. The results verified that TPT was initially adsorbed by the cell surface of *Stenotrophomonas maltophilia* and was subsequently transported and degraded intracellularly with diphenyltin and monophenyltin production. Cl^-, Na^+, arabinose and glucose release, membrane permeability and the extracellular protein concentration increased during TPT treatment, whereas K^+ and PO_4^{3-} utilization and intracellular protein concentration declined. The biosorption, degradation and removal efficiencies of TPT at 0.5 mg L^{-1} by 0.3 g L^{-1} viable cells at 10 d were 3.8, 77.8 and 86.2%, respectively, and the adsorption efficiency by inactivated cells was 72.6%.

1. Introduction

Triphenyltin (TPT) is primarily used as a fungicide, herbicide, pesticide and antifouling paint worldwide [1]. As an endocrine disruptor, TPT is detrimental to various organisms with a wide range of toxicological properties, seriously disturbing the endocrine system, preventing enzyme expression and causing reproductive toxicity [2–4]. Thus, it is necessary to remove TPT from biota, water and sediment.

TPT can be removed by biodegradation [5], photolysis [6], biological uptake [7], sedimentation and flux [8]. Biological methods with low energy or chemical requirements have recently attracted attention on increasing the biodegradation capacity of effective biomasses and revealing the biodegradation mechanisms [9,10]. However, the long half-life of TPT, varying from weeks to years, has demonstrated that it takes time for biomasses to tolerate and subsequently degrade TPT [11]. Moreover, the majority of studies merely attempting to investigate the biodegradation process have ignored the contribution of biosorption and bioaccumulation to TPT removal.

To explore the mechanisms of TPT biodegradation thoroughly, revealing the interaction between cells and TPT and further illustrating the relation among biosorption, biodegradation and bioaccumulation are necessary because biosorption is the initial reaction in TPT transport and degradation, which primarily occurs intracellularly [10]. Although biosorption is an innovative technology using biomass to remove heavy metals and dyes from wastewater, only a small number of studies have attempted to clarify organotin binding by cells. For example, the tributyltin (TBT) adsorbed by a single cell of *Pseudoalteromonas* sp. was approximately $10^{7.5}$ molecules [12]. TPT and coexisting heavy metals in

* Corresponding author. Tel.: +86 20 85226615; fax: +86 20 85226615.
E-mail addresses: jsye@jnu.edu.cn, folaye@126.com (J. Ye).

http://dx.doi.org/10.1016/j.jhazmat.2014.05.023
0304-3894/

solution could be adsorbed effectively by *Brevibacillus brevis* [10]. Subsequently, TPT transported through the cell membrane due to its hydrophobicity and metabolism, which caused intracellular accumulation and biodegradation. Because TPT transport and transformation steps are metabolically mediated activities [7,13], the limited information regarding the cellular metabolism during these processes, for example, nutrient use and ion metabolism, hinders the understanding and improvement of TPT bioremoval. Therefore, it is critical to determine the relation between degradation and cellular metabolism, verify the rate-limiting reaction, and clarify whether dearylation during TPT degradation occurs successively or synchronously. Moreover, examining material transport into and out of the cell is vital for clarifying the links among TPT lipid solubility, transmembrane transport and degradation.

Stenotrophomonas maltophilia can effectively adsorb and transform heavy metals, polycyclic aromatic hydrocarbons, insecticides or their mixtures [14]. Revealing the interactions between its physiological response and organotin treatment will accelerate the application of *S. maltophilia* on the removal of organotin in the environment, as well as various coexisting pollutants. Therefore, the *S. maltophilia* activity in TPT biosorption, biodegradation and bioaccumulation was investigated in the present study. Cl^-, SO_4^{2-}, PO_4^{3-}, Na^+, Mg^{2+}, K^+, arabinose and glucose uptake and release, total and intracellular metabolites, cellular membrane permeability and protein concentration changes during TPT treatment were also analyzed to elucidate the mechanisms of TPT biodegradation.

2. Materials and methods

2.1. Strain and chemicals

S. maltophilia was preserved in the laboratory of the School of Environment at Jinan University. This strain was isolated from the sediment samples collected at Guiyu in Guangdong Province, China. The samples contained high levels of organotins, heavy metals, polycyclic aromatic hydrocarbons and other toxic pollutants [15].

TPT was obtained from Sigma–Aldrich (St. Louis, MO, USA). The concentrations of beef extract, peptone, NaCl and $MgSO_4$ in cellular culture medium were 3, 10 and 5 g L^{-1} and 10 mg L^{-1}, respectively. The TPT treatment solution contained (in mg L^{-1}) 100 $Na_2HPO_4{\cdot}12\ H_2O$, 50 KH_2PO_4, 50 NaCl, 20 NH_4NO_3, 10 $MgSO_4$ and 10 tea saponin. Among these compounds, tea saponin was used as a carbon source and surfactant to encourage TPT emulsification and enhance TPT affinity in *S. maltophilia*.

2.2. Microbial culture

S. maltophilia was inoculated into the culture medium at 37 °C on a rotary shaker at 100 r min^{-1} for 2 d to an optical density (OD) of 1.5. Subsequently, the cells were separated by centrifugation at 3500 × *g* for 5 min and washed three times with sterile distilled water before use in further experiments. The cellular growth phases were determined by the OD at 600 nm. Briefly, cultures were diluted to an OD of less than one to fall into the linear range of measurement. The actual OD was determined by multiplying by the dilution factor. The relation between the cellular growth phases and TPT treatment was investigated by setting the culture time from 3 h to 6 d.

2.3. TPT removal, biodegradation and biosorption by S. maltophilia

The removal and biodegradation of 0.5 mg L^{-1} TPT by 0.3 g L^{-1} *S. maltophilia* were performed in the dark at 25 °C in 20 mL treatment solution shaking on a rotary shaker at 100 r min^{-1}. After treatment, cells were separated by centrifuged at 3500 × *g* for 5 min. Residual TPT in the resultant supernatant was detected to determine the removal efficacies, and the total residual TPT in the supernatant and cells was used to determine the biodegradation efficacies. To clarify the trend of TPT biosorption, the TPT-loaded cells were washed by phosphate buffer solution (PBS) for 20 min. Subsequently, TPT in PBS was detected to determine the TPT absorbed by cellular surface. Nutrient use, intracellular ions and monosaccharide released by cells, the metabolites of TPT biodegradation and the change in cellular membrane permeability were detected after degradation for 0.5 h to 10 d.

To reveal the contribution of metabolism-independent adsorption to TPT bio-removal, 0.5 mg L^{-1} TPT was treated with 0.3 g L^{-1} dead cells, which were inactivated by 2% glutaraldehyde for 24 h. After adsorption for 0.5 h to 10 d, the cells were separated by centrifugation at 3500 × *g*. The residual TPT in supernatant was detected to determine the adsorption efficacies. The controls were run in parallel in flasks with solutions that were not inoculated.

The ratios of TPT biosorption, adsorption, degradation and removal are calculated as follows:

$$Q = \frac{(C_c - C_t) \times 100}{C_c}$$

where Q represents the ratio (%), C_c stands for the TPT concentration shown in the control experiment, and C_t is the final concentration of TPT after bio-treatment.

2.4. Extraction and derivatization of extra- and intracellular phenyltins (PTs)

After degradation, 10 mL hexane was added to 20 mL treatment solution. PTs in the mixture were sonicated for 20 min in an ultrasonic bath and allowed to set until phase separation. After the organic phase was removed, 10 mL hexane was added into the aqueous phase, and the operation was repeated again. The organic part was collected, followed by concentrating using a rotary evaporator at 30 °C. The residues containing the extracellular PTs were dissolved by 5 mL methanol and derivatized in pH 4.5 acetate buffer with 2 mL of 2% sodium diethyl dithiocarbonate.

To obtain the intracellular fraction, the aqueous phase with cells was collected after the above extraction in a glass vessel and was subsequently kept in an ice bath during the cell disruption to prevent overheating. Cell disruption was performed at 650 W for 5 min. Next, the intracellular PTs were extracted and derivatized using the same methods as the extracellular ones.

2.5. Analytical methods of TPT and its metabolites

PTs were analyzed according to previously published methods by gas chromatography–mass spectrometry (GC-MS) (QP2010, Shimadzu) equipped with a type Rxi-5MS GC column (30 m × 0.25 mm × 0.25 μm) [10]. Briefly, helium at 1.1 mL min^{-1} was used as the carrier gas. The column temperature program started at 50 °C for 1.5 min. The oven was heated to 300 °C at a rate of 10 °C min^{-1} for 4 min. The solvent cut time was set to 2.6 min. Mass spectra were recorded at 1 scan s^{-1} under electronic impact with electron energy of 70 eV and mass range from 50 to 650 atoms to mass unit.

2.6. Analytical methods of ions and monosaccharides

After TPT degradation by 0.3 g L^{-1} viable cells for 0.5 h to 10 d, the treatment solutions were centrifuged at 3500 × *g* for 10 min. The resultant supernatant was filtered using a 0.22-μm polyether sulfone filter, and the concentrations of Cl^-, PO_4^{3-}, SO_4^{2-}, Na^+, K^+ and Mg^{2+} were detected by an ICS-900 ion chromatography system

(Dionex, Sunnyvale, USA). Arabinose, glucose, mycose, rhamnose, galactose, xylose, mannose and fructose were detected by an ICS-2500 ion chromatography system (Dionex, Sunnyvale, USA).

2.7. Cellular membrane permeability

Membrane permeability was determined by measuring the concentration of β-galactosidase released into the culture medium using *o*-nitrophenyl-β-D-galactoside (ONPG) as a substrate [16].

2.8. Statistical analysis

All of the experiments were performed in triplicate, and the mean values were used in the calculations. The statistical analysis of the correlation between TPT treatment and cellular physiochemical characteristics was performed by SPSS version 13.0 using Pearson correlation tests.

3. Results and discussion

3.1. Cellular growth phases and TPT treatment

The cell density in the culture medium at different culture times was detected to determine the cellular growth phase. Fig. 1a shows that there was almost no lag phase, indicating that *S. maltophilia* adapted to the environment in a short time and then grew exponentially between 3 and 26 h, followed by an apoptotic phase from the 4th day. To determine the optimal culture time to harvest cells for TPT degradation, cells cultured at different time were separated from the culture medium and were used to remove TPT in the treatment solution. The tendency of the degradation curve was similar to that of the growth curve (Fig. 1b), which implied that there was a significant correlation between TPT degradation and cellular growth. However, TPT removal did not correlate with cellular growth. The Pearson correlation analysis also demonstrated that TPT degradation had a much better correlation with cellular growth than did TPT removal ($P < 0.01$).

The above outcomes primarily resulted from the fact that TPT removal was attributed to the joint effect of biosorption, biodegradation and bioaccumulation because TPT removal in the present study was determined by the total TPT decrease from the treatment solution, which included TPT transformed to catabolites by cell metabolism, adsorbed by the cell surface, and accumulated intracellularly. TPT removal did not significantly correlate with cell growth because it depends more on metabolism-independent biosorption, which relied on the cellular binding capacity by complex processes that comprise electrostatic interactions, van der Waals forces, covalent bonding, ion exchange, extracellular precipitation, or a combination [15,17]. TPT biosorption by *B. brevis* revealed that TPT binding was a rapid process because hydrophobic TPT tends to interact with lipids and proteins, which are the primary constituents of the cellular membrane [10]. Nevertheless, TPT biodegradation depends on the activity of relevant enzymes, which are metabolism-dependent. For example, cytochrome P-450 enzymes in *Streptomyces* sp., rat, hamster, porpoise and human hepatic microsomes have been confirmed to be applicable metabolic systems for TPT and TBT biodegradation [13,18]. Cells cultivated for 2 d were used for further experiments because high cell density and optimal efficiencies of TPT degradation and removal were attained at this time.

3.2. TPT removal and biosorption

Residual TPT in the control solution was in the range of 0.91–0.96 mg L^{-1}, indicating that abiotic loss was not the main route of TPT degradation (Fig. 2a). Initially, the TPT removal efficiency by viable cells was far more significant than biodegradation, and it reached its peak value of 95.4% at 0.5 d, whereas biodegradation was still low. Subsequently, the biodegradation efficiency continued to increase to 77.8%, narrowing the gap to a small value. This finding suggests that the removal process was initially dominated by either biosorption or bioaccumulation, and biodegradation gradually prevailed. The decreasing tendency of TPT biosorption from 43.7% to 3.8% confirmed that biosorption activity removed the majority of TPT initially. Although the removal efficiency was stable around the peak value, it generally displayed a slight decline and decreased to 86.2% at the 10th d. This trend was likely caused by TPT desorption, intracellular TPT release, cellular metabolism change, or a combination. To verify this inference, TPT adsorption by dead cells inactivated by 2% glutaraldehyde for 24 h was conducted. Fig. 2b shows that 32.9% TPT was adsorbed within 0.5 h, and the adsorption efficiency slowly increased thereafter to 72.6% at the 10th d.

These results further confirmed that TPT biosorption was primarily dependent on the physicochemical interactions between TPT and *S. maltophilia*. Active sites on the cell surface for TPT binding were quickly occupied during the initial rapid phase. This is consistent with TPT biosorption by *B. brevis*, in which more than 97% TPT was adsorbed within 1 h [10]. Moreover, approximately 85–95% of TBT at 0.3 mg L^{-1} was almost instantaneously adsorbed by dead cells of *Chlorella miniata*, *Chlorella sorokiniana*, *Scenedesmus dimorphus* and *Scenedesmus platydiscus* [19]. As the cell active sites and TPT in solution decreased, the chances of residual TPT to contact cells reduced accordingly, which correlated with the subsequent slow increase in TPT biosorption with time. The results shown in Fig. 2 revealed that TPT biosorption occurred and that it played a major role in the early stage of TPT removal.

Considering that TPT adsorption by dead cells did not decline with time, surface desorption may not have contributed to the decrease of TPT removal by viable cells exhibited in Fig. 2a, suggesting that it might be the release of intracellular TPT or the changes of cell metabolism or morphology under TPT and its metabolites exposure that made the removal efficiency decline. Furthermore, the sum of the TPT biosorption and biodegradation efficiencies in Fig. 2a was significantly lower than the TPT removal efficiency, indicating the existence of TPT transport and intracellular accumulation. The following experiments separately examined the contribution of the transport, accumulation and biodegradation to TPT removal.

3.3. TPT biodegradation and bioaccumulation

Fig. 3 shows that TPT was transferred, accumulated and degraded in the cells accompanied by minimal release of TPT and its metabolites from the cell. After the rapid biosorption process, TPT was transferred across the cell membrane through active transport and interactions with the membrane [20] because TPT tends to interaction with membrane lipids and proteins. The lipophilic and ionic properties of organotins result in their accumulation in various organs. The binding of TBT and its catabolites to the membrane of *Aeromonas veronii* was found during TBT degradation [21]. The change in the TPT, diphenyltin (DPT) and monophenyltin (MPT) concentrations and their sum values (PTs) during the treatment process indicated that DPT production lagged behind TPT degradation (Fig. 3a) but responded to it followed by MPT generation. For example, a fast decreasing trend of residual TPT was observed at 0.5–12 h, whereas high levels of produced DPT in the range of 72.3–74.7 μg L^{-1} were attained at 0.5–2 d. Higher concentrations of MPT appeared at 2–5 d, indicating that the cleavage of the benzene ring occurred successively not synchronously. The slow increasing tendency of the TPT degradation speed with time correlated with the degradation of the produced metabolites and with the

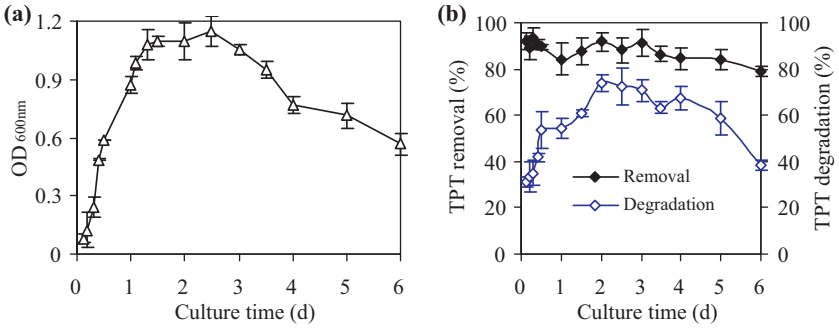

Fig. 1. Effect of culture time on biomass and treatment of 0.5 mg L^{-1} TPT by *S. maltophilia* at 25 °C for 5 d. (a) Cell density in the culture medium at different culture times; (b) TPT removal and degradation in treatment solution by cells separated at different culture times.

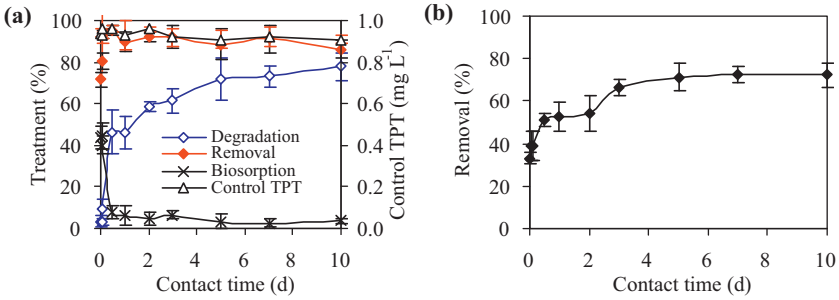

Fig. 2. Biosorption, degradation and accumulation of 0.5 mg L^{-1} TPT by *S. maltophilia* at 25 °C. (a) TPT biosorption, degradation and removal by viable cells; (b) TPT adsorption by dead cells inactivated by 2% glutaraldehyde for 24 h.

reduced contact of residual TPT with enzymes. In addition, the prolonged exposure to TPT and its metabolites might negatively affect the metabolic activity of *S. maltophilia* because TPT inhibited various organisms with its toxicological properties [2–4]. Similar to the decreasing TPT, the downward trend of PTs confirmed that a large part of TPT was transformed to inorganic tin.

The intracellular concentration of TPT within 2 h was low (Fig. 3b), but at the same time, most of the TPT had been removed from the liquid (Fig. 3a). Thus, initially TPT was mainly adsorbed by the cell surface and little was transported across the membrane. After 0.5 d, the majority of the residual TPT was detected inside *S. maltophilia*, illustrating that TPT was transferred into the cytoplasm and degraded intracellularly. The release of DPT and MPT stemmed from either active release resulting from the detoxification of PTs by living cells or from efflux from damaged or dead cells caused by PT stress. However, most of the produced DPT and MPT still accumulated in the cells, implying that bioaccumulation also partially contributed to the removal of TPT from the environment.

3.4. Nutrient utilization and ion release by cells during TPT removal

The ion concentration changes in these experiments were measured as the experimental minus the control concentrations, so a negative value meant ion use and a positive value implied ion release by *S. maltophilia*. Fig. 4 shows that Na^+ and Cl^- were released throughout the entire process, K^+ and PO_4^{3-} varied with similar trends, and SO_4^{2-} and Mg^{2+} hardly changed. The ions that exhibited an elevated trend with time implied that TPT stress increased membrane permeability or triggered apoptosis in certain cells [22].

The concentration of Na^+ and Cl^- in the cells, which were separated from the culture medium containing 5 g L^{-1} NaCl, was very high; hence, the cells were the sources of the released Na^+ and Cl^-. Cl^- uptake and release is mainly determined by the concentration gradient and regulates cellular osmotic pressure [23]. During the TPT removal process, the osmosis of the surroundings was always lower than that of the cytoplasm, as well as the exposure to PTs. Hence, Cl^- release was induced. Triorganotins mediate the

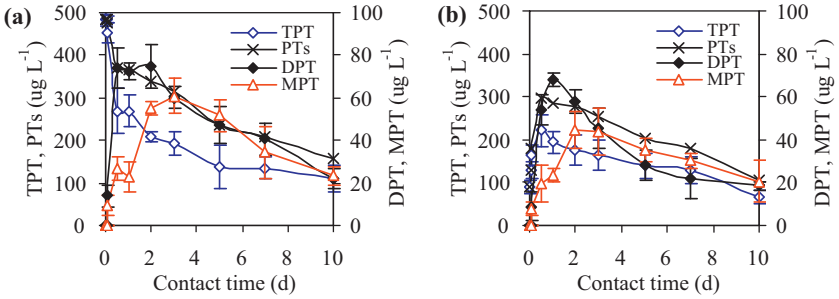

Fig. 3. Biodegradation metabolites of 0.5 mg L^{-1} TPT by *S. maltophilia* at 25 °C. (a) Total concentrations of TPT, PTs, DPT and MPT; (b) Intracellular concentrations of TPT, PTs, DPT and MPT.

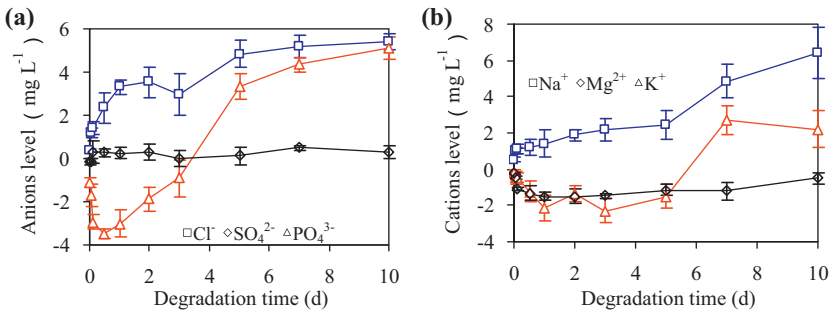

Fig. 4. Nutrient utilization and ion release by *S. maltophilia* at 25 °C during TPT removal. (a) Anion concentration change; (b) cation concentration change.

exchange diffusion of halides and other inorganic anions across biological and model membranes [24].

Combined with the K^+ variation, the joint effect of osmotic pressure, pollutant stress and Na^+/K^+ pump may explain the Na^+ curve. Na^+/K^+-ATPase is activated by binding to intracellular Na^+ and extracellular K^+ and changes the conformation to let Na^+ out and K^+ in. During this process, matter that cannot easily cross the membrane, such as TPT, enters cells by co-transport [25], which was proven by the TPT uptake exhibited in Fig. 3b. Thus, the Na^+ value was always positive, but K^+ was negative at the beginning.

After 5 d, K^+ started to exit rather than enter the cells. This was likely caused by a membrane permeability increase or release from dead cells. Na^+/K^+-ATPase transports Na^+ and K^+ in opposite directions; it does not specifically explain the sudden change. On the contrary, the fact that cell disruption or a membrane permeability increase will enhance intracellular material release explains the abrupt rise in both the Na^+ and K^+ curves.

Mg^{2+} began with increased intake and ended with relatively reduced uptake, which correlated with its functions. Mg^{2+} is an important constituent of various enzymes and can transport in association with other ions. In these ways, Mg^{2+} was assimilated more at the beginning when reactions for TPT transport, degradation and accumulation were efficient, as shown in Figs. 2a and 3b. Subsequently, the declining speed of TPT degradation was partially responsible for the decreased Mg^{2+} uptake.

The PO_4^{3-} curve stayed below the axis until 3.5 d and then rose above it. During the TPT removal process, energy is needed to transport TPT and degrade it, as well as support all types of cellular activities; hence, ATP and other P-containing polymers, which need PO_4^{3-} as a Pi source, are consumed quickly. Regarding the positive section of PO_4^{3-}, TPT stress increased membrane permeability, inducing damage and death of some cells. TPT can also alter the molecular organization of the membrane [26], triggering a spontaneous efflux of certain ions.

Sulfur, another essential element in organisms, not only exists as a structural constituent but also plays specific functions in metabolism, especially because it is embedded in certain necessary proteins [27]. The oxygenolysis of the sulfur-containing biomolecules induced by TPT, as well as the alteration in membrane permeability, may be related to the stable release of SO_4^{2-} during the degradation process.

3.5. Monosaccharide release by cells during TPT removal

Arabinose was not added to the degradation system, so its appearance in the solution could only come from the cells. Apart from cellular release, glucose might also be a metabolite of tea saponin degradation because tea saponin can serve as a nutrient for cell metabolism due to its bioavailability. Fig. 5 shows that the fastest increase of glucose and arabinose in solution was in the first 2 d, but glucose continued to be released or generated, whereas arabinose was consumed by the cells later on. In most situations, monosaccharides are easily assimilated unless the cells are abnormally influenced by stresses. Thus, monosaccharides' increasing concentrations illustrated that TPT exerted a suppressive effect on the cell membrane, driving certain intracellular monosaccharides out or inhibiting their reuse by viable cells.

The pentose phosphate pathway is the major pathway of arabinose and glucose, in which the *GAL* gene plays a dominant role in their transport [28]. In the current study, once TPT posed a detrimental effect on this pathway, these two monosaccharides were released from the cells and potentially had difficulty reentering the cells, which is reflected in the initial fast ascending tendencies of arabinose and glucose. Because transcription of the *GAL* regulon requires the presence of arabinose at a certain concentration [29], after the arabinose level reached this value, transcription of the *GAL* regulon began, triggering reuptake of the released arabinose into the cells. These findings explain the decrease in the arabinose concentration in the solution observed after 2 d (Fig. 5). Arabinose exhibits a suppressive effect on glucose uptake [30], which may partially explain the continued increase of glucose in the treatment solution during the degradation process after 2 d. Additionally, no other monosaccharides were detected, implying that TPT did not induce severe damage or apoptosis in *S. maltophilia*, which would trigger a significant efflux of other cytosolic monosaccharides.

3.6. Cellular membrane permeability

ONPG in solution cannot transport across the membrane and thus cannot induce the generation of intracellular β-galactosidase. The presence of *o*-nitrophenol in solution implies the hydrolysis of ONPG by β-galactosidase. Considering the OD value increased with time (Fig. 6), it is likely that the cell membrane altered with time; thus, ONPG could be transported into the cell,

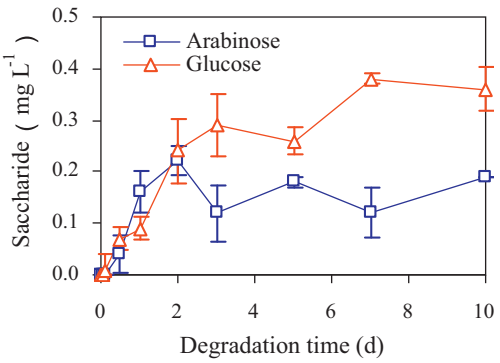

Fig. 5. Arabinose and glucose release by *S. maltophilia* at 25 °C during TPT removal.

Table 1
Correlation between TPT removal and cellular physiochemical characteristics.

Indexes	Time	Removal	Degradation	Biosorption	Na^+	K^+	Mg^{2+}	Cl^-	PO_4^{3-}	SO_4^{2-}	Permeability	Arabinose	Glucose	Extracellular protein
Removal	0.140													
Degradation	0.801*	0.525												
Biosorption	0.860*	0.462	0.966*											
Na^+	0.977*	0.181	0.748**	0.800*										
K^+	0.664**	−0.176	0.210	0.291	0.742									
Mg^{2+}	0.079	−0.859*	−0.470	−0.372	0.083	0.478								
Cl^-	0.882*	0.443	0.946*	0.948*	0.842*	0.391	−0.332							
PO_4^{3-}	0.932*	−0.099	0.647**	0.754**	0.869*	0.705**	0.265	0.770*						
SO_4^{2-}	0.437	0.703**	0.565	0.480	0.510	0.396	−0.527	0.631	0.259					
Permeability	0.974*	0.261	0.849*	0.915*	0.948*	0.627	−0.068	0.938*	0.917*	0.521				
Arabinose	0.697**	0.365	0.866*	0.767*	0.656	0.112	−0.366	0.852*	0.513	0.498	0.694**			
Glucose	0.853*	0.429	0.934*	0.948*	0.813*	0.359	−0.361	0.904*	0.743**	0.510	0.891*	0.790*		
Extracellular protein	0.474	0.579	0.850*	0.835*	0.387	−0.094	−0.678**	0.754*	0.398	0.450	0.603	0.587	0.730**	
Intracellular protein	−0.853*	−0.486	−0.828*	−0.846*	−0.870*	−0.441	0.254	−0.852*	−0.649**	−0.624	−0.850*	−0.678**	−0.775*	−0.594

* Correlation is significant at the 0.01 level (two-tailed).
** Correlation is significant at the 0.05 level (two-tailed).

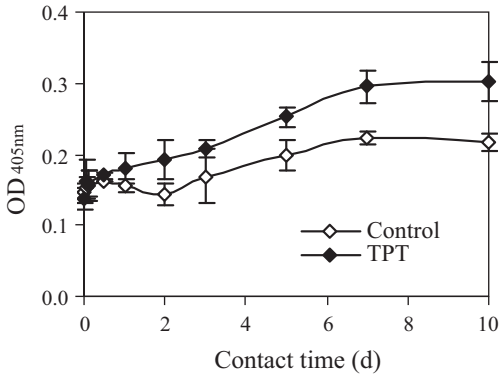

Fig. 6. Membrane permeability change of the control cells and TPT-treated cells with time.

inducing β-galactosidase and being hydrolyzed [31]. The high OD value of the TPT-treated solution confirmed that TPT, which was responsible for the increased release of ions (Fig. 4), arabinose and glucose (Fig. 5) significantly increased cell membrane permeability. Furthermore, the membrane permeability change may be one of the reasons for the partial release of intracellular PTs into the extracellular environment, as shown in Figs. 2a and 3. The membrane permeability of the control cells also increased with time but was lower than that of TPT-treated samples due to deficiency of the exotic organic nutrients in the treatment solution.

3.7. Change in the protein concentration during TPT removal

As shown in Fig. 7, the extracellular protein concentration first increased and then slightly decreased, whereas the intracellular protein level decreased gradually. Considering protein functions, as well as TPT properties, it is not difficult to explain the decreasing trend of the intracellular protein concentration. Because TPT has been reported to act as an inhibitor of some enzymes [32], this result could be attributed to TPT exposure and nutrient insufficiency in the solution, where the metabolic activity of *S. maltophilia* was repressed, reducing the biomass of living cells accordingly. Moreover, the TPT toxicity obstructs protein synthesis, changes protein structures and degrades some inactive proteins [33]. In addition, the exposure to stress, including toxic pollutants, induces the expression and transport of some proteins that are responsible for environmental adaptation [34]. Hence, the release of some proteins, induced by membrane permeability increase or environmental stress (Fig. 6), was partially related to the decrease in the intracellular proteins and the increase in extracellular proteins. With the decline of the residual TPs, fewer proteins needed to be

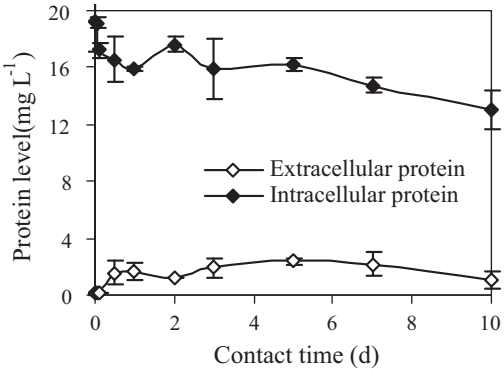

Fig. 7. Change in the intracellular and extracellular protein concentration during TPT removal.

expressed and transported to the exotic solution, thereby triggering the decrease of extracellular proteins. The reduction of intracellular proteins represented the decrease of viable cells, which was partially related to the decrease of extracellular proteins at the 10th d. The up-regulated expression of intracellular proteins at the 2nd d indicated upward cell production because of diauxic growth [35].

3.8. Correlation between TPT removal and cellular physiochemical characteristics

Consistent with the finding that the cellular membrane permeability increased with time, the correlation between the TPT treatment time and the release of intracellular materials, including Na^+, K^+, Cl^-, PO_4^{3-}, arabinose and glucose, was significant, with a p value of 0.05 or 0.01 (Table 1). The significant correlation between degradation and biosorption illustrated that TPT degradation was primarily dependent on biosorption because TPT binding by *S. maltophilia* was the initial process. Furthermore, both degradation and biosorption exhibited a significant correlation with the efflux of Na^+, Cl^-, PO_4^{3-}, arabinose, glucose and protein, the increase in membrane permeability, and the decrease in intracellular protein, revealing that TPT exposure and transformation exerted suppressive effects on cellular metabolism. However, PTs did not trigger severe damage or apoptosis in *S. maltophilia* because PTs exhibited a declining trend, Mg^{2+} was used by the cells and the intracellular protein concentration remained at a relative high level during the entire process (Fig. 7).

4. Conclusions

TPT was initially adsorbed from solution by *S. maltophilia* and was subsequently transported and intracellularly degraded with diphenyltin and monophenyltin production. After treatment for 0.5 d, residual TPT and produced diphenyltin and monophenyltin were detected intracellularly. Cl^-, Na^+, arabinose and glucose release, the cellular membrane permeability, and the extracellular protein concentration increased during TPT treatment, whereas K^+ and PO_4^{3-} utilization and the intracellular protein concentration declined. The biosorption, degradation and removal efficiencies of TPT at 0.5 mg L^{-1} by 0.3 g L^{-1} viable cells at 10 d were 3.8, 77.8 and 86.2%, respectively, and the adsorption efficiency by inactivated cells was 72.6%. These findings help to elucidate the TPT biosorption, transport and degradation mechanisms through the analysis of cellular physiological response and metabolites.

Acknowledgements

The authors would like to thank the National Natural Science Foundation of China (Nos. 21377047, 21007020), the Natural Science Foundation of Guangdong Province (No. S2013010012662), the Science and Technology Foundation of Pearl River (No. 2012J2200056), and the Major National Water Pollution Control and Management of Science and Technology Projects (No. 2012ZX07206003) for their financial support.

References

[1] F.G. Antes, E. Krupp, E.M.M. Flores, V.L. Dressler, J. Feldmann, Speciation and degradation of triphenyltin in typical paddy fields and its uptake into rice plants, Environ. Sci. Technol. 45 (2011) 10524–10530.
[2] C. Hobler, A.J.M. Andrade, S.W. Grande, C. Gericke, C.E. Talsness, K.E. Appel, I. Chahoud, K. Grote, Sex-dependent aromatase activity in rat offspring after pre- and postnatal exposure to triphenyltin chloride, Toxicology 276 (2010) 198–205.
[3] L. Yu, X.L. Zhang, J. Yuan, Q.Z. Cao, J.Q. Liu, P. Zhu, H.H. Shi, Teratogenic effects of triphenyltin on embryos of amphibian (*Xenopus tropicalis*): a phenotypic comparison with the retinoid X and retinoic acid receptor ligands, J. Hazard. Mater. 192 (2011) 1860–1868.
[4] Z.H. Zuo, C.G. Wang, M.F. Wu, Y.Q. Wang, Y.X. Chen, Exposure to tributyltin and triphenyltin induces DNA damage and alters nucleotide excision repair gene transcription in *Sebastiscus marmoratus* liver, Aquat. Toxicol. 122–123 (2012) 106–112.
[5] A.S. Stasinakis, N.S. Thomaidis, A. Nikolaou, A. Kantifes, Aerobic biodegradation of organotin compounds in activated sludge batch reactors, Environ. Pollut. 134 (2005) 431–438.
[6] W.U. Palm, R. Kopetzky, W. Ruck, OH-radical reactivity and direct photolysis of triphenyltin hydroxide in aqueous solution, J. Photochem. Photobiol. A 156 (2003) 105–114.
[7] H. Yamada, K. Takayanagi, Bioconcentration and elimination of bis (tributyltin) oxide (TBTO) and triphenyltin chloride (TPTC) in several marine fish species, Water Res. 26 (1992) 1589–1595.
[8] S. Díez, S. Lacorte, P. Viana, D. Barceló, J.M. Bayona, Survey of organotin compounds in rivers and coastal environments in Portugal 1999–2000, Environ. Pollut. 136 (2005) 525–536.
[9] J. Heroult, Y. Nia, L. Denaix, M. Bueno, G. Lespes, Kinetic degradation processes of butyl- and phenyltins in soils, Chemosphere 72 (2008) 940–946.
[10] J.S. Ye, H. Yin, H. Peng, J.Q. Bai, D.P. Xie, L.L. Wang, Biosorption and biodegradation of triphenyltin by *Brevibacillus brevis*, Bioresour. Technol. 129 (2013) 236–241.
[11] L.Ó. Guðmundsdóttir, K.K.Y. Ho, J.C.W. Lam, J. Svavarsson, K.M.Y. Leung, Long-term temporal trends (1992–2008) of imposex status associated with organotin contamination in the dogwhelk *Nucella lapillus* along the Icelandic coast, Mar. Pollut. Bull. 63 (2011) 500–507.
[12] H. Mimura, R. Sato, Y. Furuyama, A. Taniike, M. Yagi, K. Yoshida, A. Kitamura, Adsorption of tributyltin by tributyltin resistant marine *Pseudoalteromonas* sp. cells, Mar. Pollut. Bull. 57 (2008) 877–882.
[13] J. Yang, Y. Oshima, I. Sei, N. Miyazaki, Metabolism of tributyltin and triphenyltin by Dall's porpoise hepatic microsomes, Chemosphere 76 (2009) 1013–1015.
[14] S.N. Chen, H. Yin, J.S. Ye, H. Peng, Z.H. Liu, Z. Dang, J.J. Chang, Influence of co-existed benzo[a]pyrene and copper on the cellular characteristics of *Stenotrophomonas maltophilia* during biodegradation and transformation, Bioresour. Technol. 158 (2014) 181–187.
[15] J.S. Ye, H. Yin, D.P. Xie, H. Peng, J. Huang, W.Y. Liang, Copper biosorption and ions release by *Stenotrophomonas maltophilia* in the presence of benzo[a]pyrene, Chem. Eng. J. 219 (2013) 1–9.
[16] H.R. Ibrahim, Y. Sugimoto, T. Aoki, Ovotransferrin antimicrobial peptide (OTAP-92) kills bacteria through a membrane damage mechanism, Biochim. Biophys. Acta 1523 (2000) 196–205.
[17] Y.Q. Tao, W. Li, B. Xue, J.C. Zhong, S.C. Yao, Q.L. Wu, Different effects of copper (II), cadmium (II) and phosphate on the sorption of phenanthrene on the biomass of cyanobacteria, J. Hazard. Mater. 261 (2013) 21–28.
[18] P. Bernat, J. Długoński, Isolation of *Streptomyces* sp. strain capable of butyltin compounds degradation with high efficiency, J. Hazard. Mater. 171 (2009) 660–664.
[19] N.F.Y. Tam, A.M.Y. Chong, Y.S. Wong, Removal of tributyltin (TBT) by live and dead microalgal cells, Mar. Pollut. Bull. 45 (2002) 362–371.
[20] A. Ortiz, J.A. Teruel, F.J. Aranda, Effect of triorganotin compounds on membrane permeability, BBA - Biomembranes 1720 (2005) 137–142.
[21] A. Cruz, T. Caetano, S. Suzuki, S. Mendo, *Aeromonas veronii*, a tributyltin (TBT)-degrading bacterium isolated from an estuarine environment, Ria de Aveiro in Portugal, Mar. Environ. Res. 64 (2007) 639–650.
[22] Y. Miura, H. Matsui, Effects of triphenyltin on cytosolic Na^+ and Ca^{2+} response to glucose and acetylcholine in pancreatic β-cells from hamster, Toxicol. Appl. Pharmacol. 174 (2001) 1–9.
[23] Q. Zhao, K. Ovchinnikova, B.H. Chai, H. Yoo, J. Magula, G.H. Pollack, Role of proton gradients in the mechanism of osmosis, J. Phys. Chem. B 113 (2009) 10708–10714.
[24] J. Gabrielska, T. Kral, M. Langner, S. Przestalski, Different effects of di- and triphenyltin compounds on lipid bilayer dithionite permeabilization, Z. Naturforsch. C 55 (2000) 758–763.
[25] M. Sopjani, I. Alesutan, J. Wilmes, M. Dërmaku-Sopjani, R.S. Lam, E. Koutsouki, M. Jakupi, M. Föller, F. Lang, Stimulation of Na^+/K^+ ATPase activity and Na^+ coupled glucose transport by β-catenin, Biochem. Biophys. Res. Commun. 402 (2010) 467–470.
[26] D. Bonarska-Kujawa, H. Kleszczyńska, S. Przestalski, The location of organotins within the erythrocyte membrane in relation to their toxicity, Ecotoxicol. Environ. Saf. 78 (2012) 232–238.
[27] P.M. Matias, I.A.C. Pereira, C.M. Soares, M.A. Carrondo, Sulphate respiration from hydrogen in *Desulfovibrio* bacteria: a structural biology overview, Prog. Biophys. Mol. Biol. 89 (2005) 292–329.
[28] H.W. Wisselink, C. Cipollina, B. Oud, B. Crimi, J.J. Heijnen, J.T. Pronk, A.J.A. van Maris, Metabolome, transcriptome and metabolic flux analysis of arabinose fermentation by engineered *Saccharomyces cerevisiae*, Metab. Eng. 12 (2010) 537–551.
[29] S.K. Upadhyay, Y.U. Sasidhar, Molecular simulation and docking studies of Gal1p and Gal3p proteins in the presence and absence of ligands ATP and galactose: implication for transcriptional activation of *GAL* genes, J. Comput. Aided Mol. Des. 26 (2012) 847–864.
[30] K. Shibanuma, Y. Degawa, K. Houda, Determination of the transient period of the EIS complex and investigation of the suppression of blood glucose levels by L-arabinose in healthy adults, Eur. J. Nutr. 50 (2011) 447–453.
[31] G.Y. Shi, H. Yin, J.S. Ye, H. Peng, J. Li, C.L. Luo, Effect of cadmium ion on biodegradation of decabromodiphenyl ether (BDE-209) by *Pseudomonas aeruginosa*, J. Hazard. Mater. 263 (2013) 711–717.

[32] S. Lo, I. King, A. Alléra, D. Klingmüller, Effects of various pesticides on human 5α-reductase activity in prostate and LNCaP cells, Toxicol. In Vitro 21 (2007) 502–508.
[33] G. D'Onofrio, F. Tramontano, A.S. Dorio, A. Muzi, V. Maselli, D. Fulgione, G. Graziani, M. Malanga, P. Quesada, Poly (ADP-ribose) polymerase signaling of topoisomerase 1-dependent DNA damage in carcinoma cells, Biochem. Pharmacol. 81 (2011) 194–202.
[34] L.Q. Su, C.H. Xu, R.W. Woodard, J. Chen, J. Wu, A novel strategy for enhancing extracellular secretion of recombinant proteins in *Escherichia coli*, Appl. Microbiol. Biotechnol. 97 (2013) 6705–6713.
[35] A.I. Casasús, R.K. Hamilton, S.A. Svoronos, B. Koopman, A simple model for diauxic growth of denitrifying bacteria, Water Res. 39 (2005) 1914–1920.